Green Chemistry

Selective Hydrothermal Reductions Using Geomimicry

SCHOLARONE™
Manuscripts

Selective Hydrothermal Reductions Using Geomimicry

Christiana Bockisch,[a] Edward D. Lorance,[b] Garrett Shaver,[a] Lynda B. Williams,[c] Hilairy E. Hartnett,*[ac] Everett L. Shock,*[ac] and Ian R. Gould*[a]

[a] *School of Molecular Sciences, Arizona State University, Tempe, AZ 85287*

[b] *Department of Chemistry, Vanguard University, Costa Mesa, CA 92926*

[c] *School of Earth and Space Exploration, Arizona State University, Tempe, AZ 85287*

Abstract

Reduction of carbon-carbon π-bonds has been demonstrated using iron powder as the reductant and simple powdered nickel as the catalyst in water as the solvent at 250°C and the saturated water vapor pressure, 40 bars. Stereochemical, kinetic and electronic probes of the mechanism suggest reaction *via* a conventional Horiuti-Polyani process for hydrogenation at the nickel metal surface. Selective reduction of carbon-carbon π-bonds is observed in the presence of other functional groups. The reactions use benign and Earth-abundant reagents that are at low depletion risk and take place in water as the only solvent under conditions that are characteristic of many geochemical processes.

Introduction

The vast majority of the Earth's organic carbon is located within the crust, mainly in continental margin sediments and sedimentary basins.[1] The chemical reactions of this organic material are involved in a wide range of important geo- and biogeochemical processes, from petroleum generation to supporting subsurface microbial communities.[2] Organic reactions under these conditions are noteworthy in that they take place in water as the only solvent and use reagents and catalysts that by definition are mainly benign and Earth-abundant.[3,4] For these reasons, organic reactions under conditions that mimic geochemical conditions, i.e. geomimicry, are attracting increasing attention for green chemistry applications.[5]

Geochemically relevant temperatures are not extreme, usually well below the critical point of water, i.e. ~150°C - ~250°C. Nevertheless, water at these temperatures and associated confining pressures exhibits several characteristics that are beneficial to green chemistry applications. First, the dielectric constant is considerably lower than at room temperature: at 250 °C, close to those of methanol and acetone (~25), thus water at these temperatures is a good solvent for many organic compounds.[6] Second, the pK_W of water at 250°C is 11 compared to the canonical 14 at 25°C, *i.e.*, which means that the concentration of both hydronium and hydroxide ions are higher.[7] Water at these temperatures thus has "built-in" potent homogeneous acid and base catalysts in the form of H_3O^+ and ^-OH. The separation of products is also relatively easy under hydrothermal conditions because upon cooling the water, non-polar organic products will mainly separate from the water and simply float to the top. Hydrothermal conditions support a wide range of organic transformations, many of which occur in water alone, without the addition of any other reagents or catalysts,[3,4,8] or they use only benign or Earth abundant

2

reagents.[9]

Some hydrothermal reactions are unexpected, or even quite different from those described in traditional organic chemistry textbooks. For example, the dehydration of alcohols to form alkenes occurs quickly, without the need to add any reagents or catalysts, and with high chemical yield, even though organic chemistry textbooks report that under conditions closer to ambient the reaction proceeds in the reverse direction; i.e., water adds to alkenes to form alcohols.[10] We showed recently that selective organic oxidation reactions could be performed under hydrothermal conditions using the extremely mild oxidizing agent copper(II).[9] Hydrothermal oxidation of a primary alcohol to an aldehyde was accomplished with Cu(II), with minimal further oxidation to the carboxylic acid, even though water was the solvent.[9] Oxidation reactions are among the most frequently studied in green chemistry contexts;[11] in contrast, organic reductions have received somewhat less attention. There is considerable interest in green reduction reactions; for example, in liquid fuel generation and deoxygenation,[12] and conversion of carbon dioxide into useful raw materials.[13] Reduction by catalytic hydrogenation is widely employed in traditional benchtop and industrial organic chemistry.[14] Although well established, the traditional methods for heterogeneous hydrogenation generally use rare and expensive metal catalysts such as platinum and palladium that carry a high depletion risk.[15] The traditional methods also usually use molecular hydrogen as the reducing agent.[14,16] Several alternate methods for performing catalytic reduction have been described in the literature, most of which have focused on replacing the expensive catalysts (see, for example, refs 17). However, molecular hydrogen is not naturally abundant, and is usually produced industrially from fossil fuels *via* steam reformation, a process that has significant energy cost and forms carbon dioxide as a by-product.[18] Hydrogen is also a flammable gas with storage and transportation constraints.

Therefore, there has also been considerable interest in exploring other reducing agents as alternatives to molecular hydrogen.[19]

Of particular interest in this regard is a recent communication in this journal by Schafer et al., who demonstrated selective reduction of organic functional groups using palladium on carbon as the catalyst, but using metallic aluminum as the reducing agent instead of hydrogen gas, and water as the solvent.[20] Reduction of C=C, C=N, C=O and N=O bonds was accomplished in addition to hydrogenolysis of C-O, C-N and C-X bonds. These reductions are interesting because they eliminate the need for hydrogen gas, and use water as the solvent, although the catalyst is still based on the expensive palladium metal.[20]

As part of a research program on hydrothermal organic reactions relevant to geochemical processes,[3,8-10] we have discovered several organic reduction reactions related to those reported by Schafer et al.,[20] that take place in hydrothermal water as the only solvent, that require only simple powdered nickel as the catalyst and an even milder and less-expensive reducing agent, metallic iron, avoiding the expensive palladium. Metallic iron has been extensively investigated as a reagent for large-scale industrial processes and waste remediation,[21] but reports of its use as an organic reducing agent are rare.[22] Here we describe experiments that probe the scope, selectivity, and mechanism of this new system for reducing carbon-carbon π-bonds.

Experimental

Materials

All chemical materials were obtained from Sigma-Aldrich, except 1,2-dimethylcyclohexene and 2-methyl-1-methylenecyclohexane, which were obtained from ChemSampCo. The 1,2-dimethylcyclohexene was purified by microscale distillation. Metal powders were obtained as

nickel nanopowder (two purchases of different lot numbers), and iron powder (micron sized).

Water for all experiments was 18.2 MΩ, obtained from a Barnstead™ purification system.

Methods

Metal Powder Characterization. The surface area of the nickel nanopowders was measured

using the nitrogen adsorption Brunauer–Emmett–Teller method. The surface area of the first lot

of nickel purchased was found to be 0.94±0.01 m^2/g, the second lot of nickel from the same

supplier was found to have a surface area of 3.52±0.02 m^2/g.

Powder X-ray diffraction (XRD) was performed using a Siemens D5000 with a cobalt

anode, scanned from 20° to 90° (2θ). Co-Kα radiation (40 kV, 30 mA). Three full scans were

typically averaged to increase the signal/noise ratio. Where appropriate, samples were milled to

ca. 20 micron particle size before analysis. XRD patterns were analyzed using EVA™

interpretative software and the JCPDS database (MaterialsData.com). The nickel and iron

samples were also imaged using scanning electron microscopy (SEM). Each sample was

sputtered with gold to obtain 3-5 nm coating prior to imaging with an XL30 environmental

scanning electron microscope (ESEM) with field emission gun (FEG). SEM images of each

metal powder are provided in the Supplementary Information.

Hydrothermal Experiments. Hydrothermal reactions were performed in sealed quartz/fused

silica tubes (Technical Glass Products) that were approximately 20 cm long, with 0.6 cm external

diameter and 0.2 cm internal diameter. Each reaction was performed with 0.2 g of water and the

concentrations of the organic reactants were all 0.1 molal. In each experiment, 40μmol organic

per 0.02 m^2 of Ni and 240μmol of Fe were used. To maintain a constant surface area, the mass of

the nickel was adjusted to account for the different surface areas for the two lots of the powdered nickel. After correcting for the different surface areas, there was no detectable difference between the different lots of nickel.

To eliminate oxygen, all water, liquid reagents and solutions of soluble organics in water were purged with UHP Argon for 1 hour before being added to the reaction tubes. The tubes were purged with UHP argon for an additional 10 minutes before freezing in liquid nitrogen and evacuating to 60-70 mTorr, followed by sealing with a hydrogen torch. Roughly 50% of the volume in each tube at room temperature was sample, the rest was headspace. For reactions longer than 2 hours, tubes were heated in a repurposed, preheated, gas chromatography oven. For reactions shorter than 2 hours, a brass block, equipped with internal heating elements, was used, because it allowed for much more rapid warm-up of the samples. The reactions were quenched at the end of the desired time period by plunging the tubes into room temperature water. The reactions were heated to a temperature of 250°C. Under these conditions the reaction pressure can be estimated as the saturated water vapor pressure, i.e., 40 bar.[7] This is only an estimate since if any gases are formed, see further below, the pressure in the tubes will be higher than this value.

At the end of the experiments, after heating and quenching, the tubes were frozen in liquid nitrogen, and after opening, the organic material was extracted using 2 mL of dichloromethane containing decane. The decane was used as an internal gas chromatography standard. Quantitative gas chromatography was performed using a Bruker-Scion 456 gas chromatograph equipped with a flame ionization detector. Products were quantified using calibration curves determined using authentic standards. Benzene and cyclohexane were not separable by gas chromatography, nor were the hexane isomers formed via reduction of 3-hexyne. Therefore,

experiments starting with benzene and 3-hexyne were analyzed by ^{1}H NMR using a Bruker 400 MHz instrument. The chemical yields for the reaction times indicated were characterized using quantitative gas chromatography, by comparing the calibrated peak sizes for the products to the calibrated peak size for the unreacted starting material. The mass reaction mass balances determined this way were all greater than 90% for all reactions, i.e., side products comprised less than 10% of the final reaction mixtures.

Molecular hydrogen generation was measured by opening a reaction tube in a 1 inch internal-diameter Tygon tube capped with rubber septa. The volume of the Tygon tube with the glass tube inside was determined by weighing the entire apparatus with and without water. The reaction tubes were broken in the sealed Tygon tube, and 10 μL of the headspace was quickly sampled using a gas-tight syringe and analyzed using a reducing compound photometer gas chromatograph (RCP-GC), that was calibrated with a 50 ppm H_2 standard with nitrogen balance (Praxair). The volume of the Tygon tubing and the solubility constant for hydrogen in water at 25°C, determined using the revised Helgeson-Kirkham-Flowers equations of state,[23] were used to calculate the total mass of hydrogen generated in the reaction tubes.

Results and Discussion

Reduction of Cyclohexene

Cyclohexene was studied as an example alkene. Reaction of cyclohexene in water at 250°C with nickel and iron results in 95% conversion of the alkene in 1 hour. The major product is cyclohexane (90%) plus a small amount of benzene (10%), eq 1. Cyclohexane is presumably

$$\text{cyclohexene} \xrightarrow[\text{250°C, 2 hrs}]{\text{Fe/Ni H}_2\text{O}} \text{cyclohexane} + \text{benzene} \qquad (1)$$

90%   10%
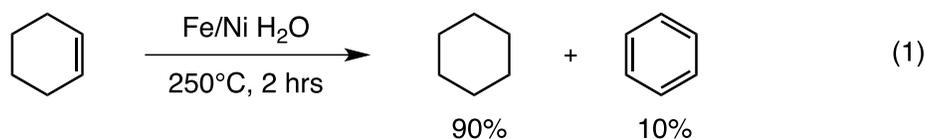
formed by hydrogenation of the alkene on the nickel surface (see below), with the hydrogen

produced from H_2O upon oxidation of the iron. Further experiments were performed in order to

investigate the roles of the nickel and the iron.

Reaction of cyclohexene was compared in reactions with nickel alone, with iron alone and

with both metals present. With both metals at 250°C the cyclohexene conversion was found to be

55% after 5 minutes. Under the same conditions and same reaction time period with nickel alone,

the conversion was 25%. This experiment shows that nickel alone is capable of reducing the

cyclohexene, with nickel presumably acting as both the reducing agent and catalyst. With iron

alone for the same time period, cyclohexene conversion was negligible (<1%). These results

suggest that metallic nickel is required in order to catalyze reduction, and that neither metallic

iron or its oxidized forms are capable of catalyzing the reaction. Additional insight was obtained

from experiments in which the possible formation of molecular hydrogen was investigated using

thermodynamic computations and experiments.

To test for formation of molecular hydrogen, a sample tube was loaded with nickel, iron, and

water, as per a typical experiment, but no organic was added. The tube was heated at 250°C for 1

hour. No attempt was made to run the reaction to completion, since the reaction tubes are at risk

of breaking due to the increased pressure when no organic molecule is present to react with any

hydrogen produced. The headspace gas was sampled as described in the experimental section

and a total of 0.12 mg of molecular hydrogen was measured, corresponding to 2.8×10^{-4} molal

aqueous hydrogen at the experimental conditions. The reaction conditions evidently produce

molecular hydrogen *in situ*, but because the extent of conversion of the iron is not accurately known the chemical yield of hydrogen cannot be determined.

Calculations based on thermodynamic parameters for nickel and iron in water were also performed to gain insight into the thermodynamic stability of the metals under the experimental conditions. The redox reactions considered, together with their equilibrium constants at 250°C are given in Scheme 1.[24-26] Magnetite, Fe_3O_4, and nickel oxide, NiO, were chosen as representative metal oxidized species for this analysis. The revised Helgeson-Kirkham-Flowers equation of state[23] was used to generate an equilibrium nickel and iron stability field diagram as a function of temperature and activity of aqueous hydrogen, Figure 1. For 240 µmol iron, and allowing 100% conversion to magnetite and hydrogen, the thermodynamic calculations predict oxidation of iron accompanied by the formation of 320 µmol of hydrogen. This hydrogen will speciate between the aqueous and gas phases. Using the known equilibrium constant for this speciation, Scheme 1, this results in 0.0039 molal hydrogen in the aqueous phase, indicated by the closed circle in Figure 1. For a system of Fe, Ni, Fe_3O_4 and NiO with this quantity of hydrogen, the thermodynamic equilibrium situation is characterized by complete essentially oxidation of iron and no oxidation of nickel.

XRD analysis was performed on the solid products obtained after reaction of a mixture of 170µmol of nickel and 450µmol of iron, at 250°C for 1 hour, 40 hour and 68 hour reaction periods in the absence of any organic. The solid products comprised a mixture that potentially contained unreacted iron, unreacted nickel and the oxidized metal products. Nickel and iron have overlapping peaks in XRD around 51°, Figure 2A. The solid products obtained from both the 1 hour and the 68 hour reactions had a broad peak in this region, Figure 2A, implying the presence of unreacted nickel and/or iron in both samples. The earlier 1 hour reaction XRD pattern more

$$\text{Ni} + \text{H}_2\text{O} \longrightarrow \text{NiO} + \text{H}_2 \qquad \text{Log } K_{250} = \text{-3.79}$$

$$3\,\text{Fe} + 4\,\text{H}_2\text{O} \longrightarrow \text{Fe}_3\text{O}_4 + 4\text{H}_2 \qquad \text{Log } K_{250} = 2.36$$

$$\text{H}_2(\text{aq}) \longrightarrow \text{H}_2(\text{g}) \qquad \text{Log } K_{250} = 2.63$$
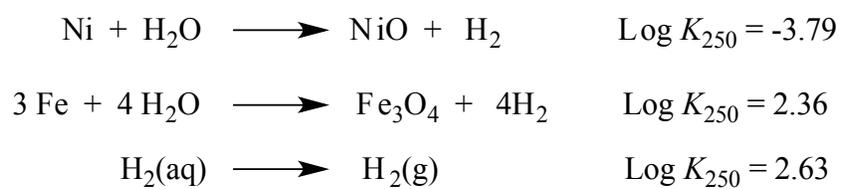
Scheme 1. Redox and other equations and their equilibrium constants at 250°C and 40 bar used in the calculation of the iron/nickel in water stability field diagram of Figure 1.
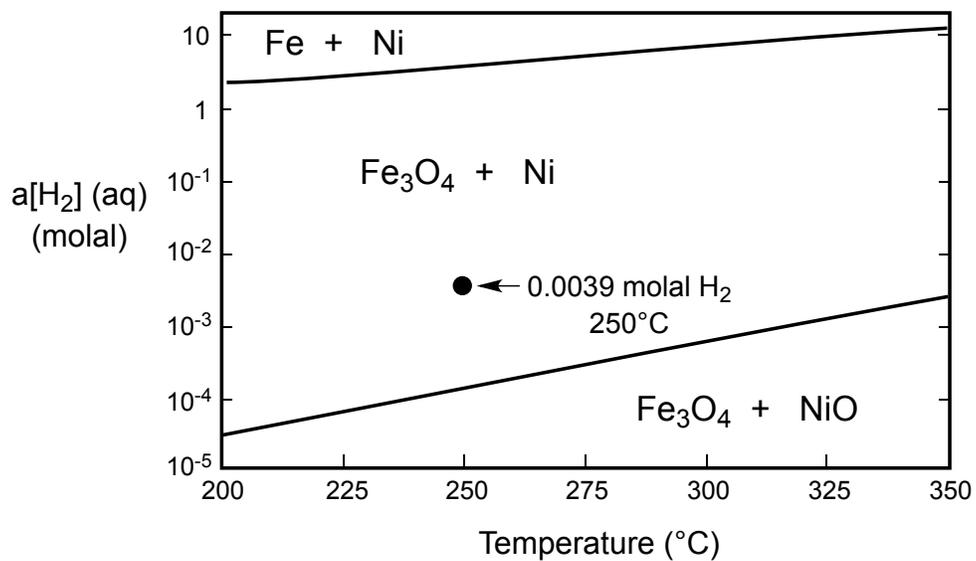
Fig 1. The stability fields of nickel, iron, iron oxide (Fe_3O_4) and nickel oxide (NiO), with respect to temperature and activity of aqueous hydrogen. The calculated maximum concentration of dissolved hydrogen for the hydrothermal experiments is indicated by the closed circle.
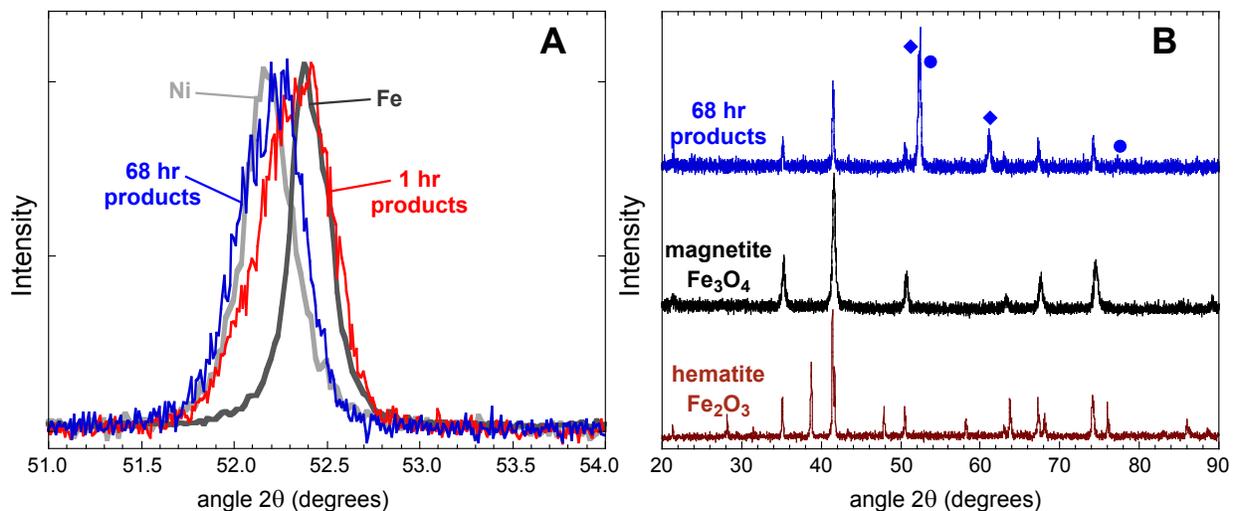
Fig 2 (**A**) XRD patterns collected using Co-kα radiation for (blue) the solid products of reaction

of nickel and iron for 68 hours at 250°C, (lighter grey) unreacted nickel powder, (darker grey)

unreacted iron powder, (red) the solid products of reaction of nickel and iron for 1 hour at 250°C.

The peaks are normalized to their maximum intensities. (**B**) XRD pattern for (upper blue) the

solid products of reaction of nickel and iron for 68 hours at 250°C, (middle black) a magnetite

(Fe_3O_4) standard, (lower brown) a hematite (Fe_3O_4) standard. The peaks indicated by diamond

symbols are associated with metallic nickel, the peaks indicated by circles are associated with

metallic iron.

closely resembles that of iron, which is expected since there is more iron than nickel in starting

mixture, Figure 2A. After 68 hours, however, the XRD pattern more closely resembles that of

nickel, Figure 2A (complete XRD patterns are provided as Supplementary Information). This is

consistent with more rapid consumption (oxidation) of iron compared to nickel under the

experimental conditions over 68 hours. New peaks are found in the XRD patterns of the reaction

products, Figure 2B. Compared to the combined iron/nickel peak at 51°, the intensities of these

new peaks are higher for the 68 hour reaction than for the 1 hour reaction, consistent with more

oxidation of the metals to generate more product at the longer reaction time. The new peaks are a

close match to those of authentic magnetite and not to hematite, Figure 2B. Analysis of samples

that were milled to 20 μm using EVA and the JCPDS database identified magnetite as the only

XRD detectable product (see Supplementary Information). Although the chemical yield of

magnetite cannot be determined from these experiments, these results strongly suggest oxidation

of iron under the experimental conditions to form molecular hydrogen and magnetite.

XRD analysis of a corresponding reaction of iron alone at 250°C for 70 hours (with no

nickel) gave product peaks identical to those from the nickel/iron experiments that were assigned

to magnetite. Reaction of nickel alone for 70 hours (with no iron) gave peaks corresponding to

unreacted nickel only, with no other XRD detectable reaction products on this timescale.

The cyclohexene reduction experiments, the measurements of hydrogen production, the XRD

product analyses and the thermodynamic calculations in Figure 1 together are consistent with

reaction in which metallic iron reacts with water to produce hydrogen and magnetite as reduction

and oxidation products, respectively, with catalytic reaction of molecular hydrogen with the

alkene occurring at the surface of metallic nickel. Nickel does not appear to oxidize under the

experimental conditions, consistent with the predictions of the thermodynamic calculations

(Figure 1). As described in more detail below, catalytic activity is maintained even over very long reaction time periods, which is also consistent with preservation of metallic nickel under the reaction conditions.

Small amounts of an oxidized product benzene were also observed in the cyclohexene reduction experiments. This is not entirely unexpected since the benzene is observed to form only at very early reaction times, i.e., presumably before build-up of appreciable hydrogen concentration *via* iron oxidation. Many hydrogenation catalysts are also dehydrogenation catalysts.[27]

Reaction Stereochemistry

Reduction of cyclohexene does not provide information about the detailed mechanism of the hydrogen addition reaction. Stereochemistry is frequently used as a probe for the mechanisms of surface catalyzed reactions;[16] therefore, 1,2-dimethylcyclohexene was studied since the reduction products in this case are different if addition occurs to the same face (which gives *cis*-1,2-dimethylcyclohexane as the product) or different faces (which gives *trans*-1,2-dimethylcyclohexane as the product) of the double bond. Nickel and nickel alloys have previously been shown to exhibit preferential formation of *cis*-isomers in the reduction of 1,2-dimethylcycloalkenes at temperatures closer to ambient, consistent with *syn*-addition of H_2.[28] 1,2-Dimethylcyclohexene was therefore studied as a stereochemical probe for hydrothermal reduction. Reaction of 1,2-dimethylcyclohexene was performed with both nickel and iron at
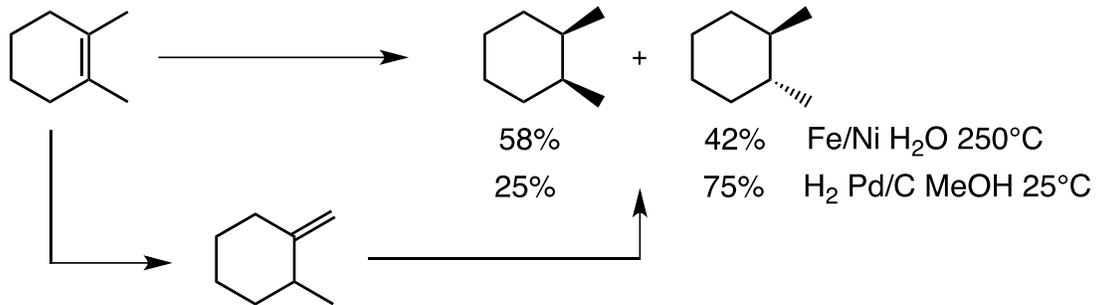
Scheme 2 Products from hydrothermal reduction of 1,2-dimethylcyclohexene with iron and nickel at 250°C after 30 min compared to corresponding reduction at room temperature (25°C) with hydrogen and Pd/C. The alkene isomer 2-methylene-1-methylcyclohexane is observed at short reaction times under both sets of conditions.

250°C. The reaction was quenched after 30 minutes in order to identify the primary reaction products. *Cis*- and *trans*-1,2-dimethylcyclohexane were formed in a ratio of 58:42 under these conditions, Scheme 2. This suggest that the reaction occurs primarily by *syn*-addition, but the preference for the *cis*-isomer is only slight, suggesting other possible competing processes. The *trans*-isomer cannot be a secondary product formed by isomerization of the *cis*-isomer. Reaction of *cis*-1,2-dimethylcyclohexane under the same conditions results in less than 1% isomerization to the *trans*-isomer on a timescale of 30 minutes.

Reduction of 1,2-dimethylcyclohexene was also performed using a conventional Pd/C catalyst with molecular hydrogen in methanol at room temperature. In this case, 1,2-dimethylcyclohexanes were formed in a *cis*-/*trans*- ratio of 25:75, i.e., the major product under these conditions is the *trans*-isomer and the product of *syn*-addition is minor. With Pd/C and molecular hydrogen at room temperature, a sample of the products was also taken at a very early reaction time, 5 seconds, after which time 4% conversion of the alkene was observed. The products observed at this very short time were the *cis*- and *trans*-1,2-dimethylcyclohexanes formed in the same 25:75 ratio as at higher alkene conversions. However, the major product at this short reaction time, 80% of the product mixture, was an isomer of the starting alkene, 2-methylene-1-methylcyclohexane, Scheme 2. This strongly suggests that alkene isomerization competes with hydrogenation. Isomerization of 1,2-dimethylcyclohexene in the presence of palladium has previously been reported by Nishimura et al.[29] Importantly, *syn*-addition of H_2 to this exocyclic alkene would be expected to form the more stable *trans*-1,2-dimethylcyclohexane. The reliability of 1,2-dimethylcyclohexane as a stereochemical probe in the Pd/C reduction is thus compromised by the formation of alkene isomers.

Hydrothermal reduction of 1,2-dimethylcyclohexene with nickel and iron at 250°C was also sampled at a reaction time with low conversion (30 minutes, 10% conversion). Similar to the Pd/C reduction, 2-methyl-1-methylenecyclohexane was also observed as the major early-time product in addition to the 1,2-dimethylcyclohexane isomers, suggesting alkene isomerization occurs under these conditions as well. In addition, small quantities of alcohols and other alkene isomers (9% of the total product mixture) were observed, presumably formed by reversible addition of water to an alkene. Dehydration of these alcohols occurs rapidly under the reaction conditions,[10] and alcohols are not observed at greater alkene conversions, nevertheless, hydration followed by dehydration represents another potential mechanism for isomerization. We conclude that alkene isomerization either directly on the nickel surface, or by hydration/dehydration, competes with *syn*-addition of hydrogen to alkenes under the reaction conditions, and that these isomerization reactions significantly reduce the stereospecificity of the reaction.

Alkyne Reduction

To further explore the scope of the reduction reactions, and in an attempt to find a better stereochemical probe of the reaction stereochemistry, two different alkynes were reduced. Reaction of diphenylacetylene (**DPA**) at 250°C with nickel and iron gave a mixture of *cis*- and *trans*-stilbene in an 80:20 ratio at all reaction times, from 5 minutes to 60 minutes. This observation is consistent with mainly *syn*-addition of H_2 since addition to the same face of the alkyne forms the less stable *cis*-isomer. The *trans*-stilbene product is likely to be a primary product rather than a secondary product formed *via* isomerization of the *cis*-stilbene, since reaction of *cis*-stilbene under the same conditions for 5 minutes resulted in less than 1% isomerization to the *trans*-isomer. As expected from the cyclohexene reduction

1
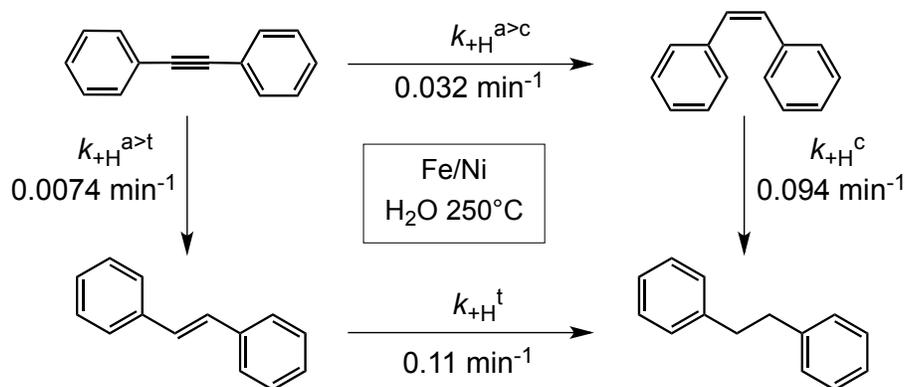
Scheme 3 Reaction pathways and pseudo-first order rate constants used to fit the time-dependent data for hydrothermal reduction (addition of hydrogen) of diphenylacetylene (a) with iron and nickel at 250°C, to form *cis*-stilbene (c) and *trans*-stilbene (t), and their follow-up reductions, see Fig 3. The uncertainties in the rate constants are estimated to be ±15%, based on repeated measurements.

1
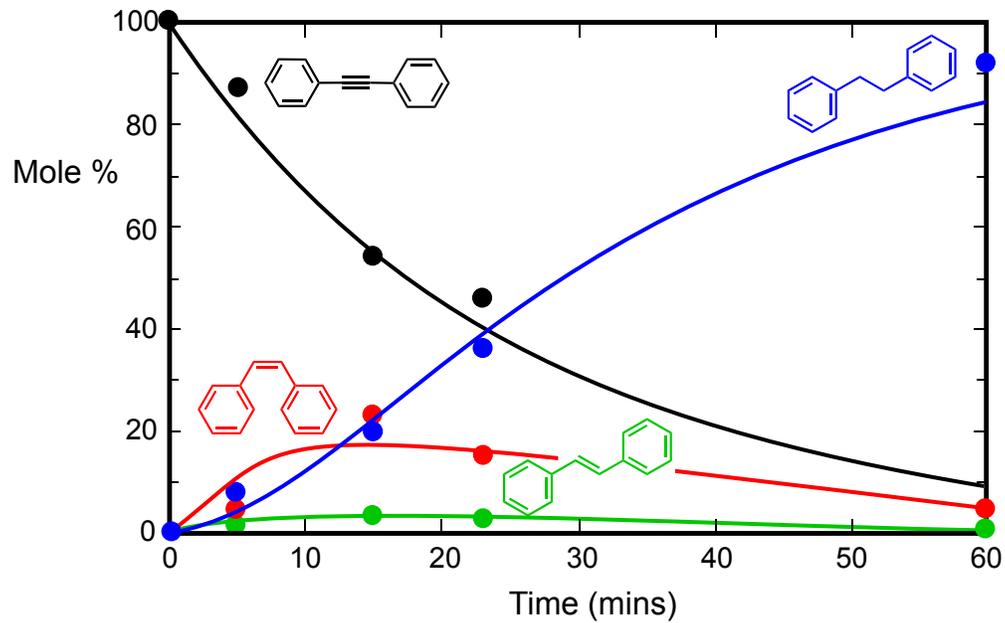
Fig 3 Time dependence of the relative concentrations or reactant and products for hydrothermal reduction of diphenylacetylene with iron and nickel at 250°C. The solid lines represent the best fits to the data according to the kinetic scheme and rate constants shown in Scheme 3.

1

experiments, the stilbene products of this reaction are eventually further reduced to bibenzyl after 1 hour, at which point essentially 100% conversion from **DPA** to bibenzyl is achieved. In order to determine the relative reactivities of the C-C double and triple bond π-systems we conducted a detailed kinetic analysis of time-dependent data.

Concentration versus time data are shown in Figure 3 for **DPA**, the two stilbene isomers and the final product biphenyl. The time-dependence of these four species was fitted to the kinetic scheme summarized in Scheme 3 using the COPASI software package.[30] The best global kinetic fit to the data is shown in Figure 3 and the corresponding values for the adjustable parameter pseudo-first order rate constants are summarized in Scheme 3. To determine the best fit values of the rate constants, minimization of error was performed using both the Levenberg/Marquardt and simulated high-temperature annealing algorithms. Error minimization was also performed using different starting values for the rate constants.

The overall rate constant for reduction of the alkyne, given as the sum of $k_{+H}^{a>c}$ and $k_{+H}^{a>t}$, is roughly one order of magnitude smaller than the rate constants for reduction of the *cis*- and *trans*- alkene isomers, k_{+H}^{c} and k_{+H}^{t}, respectively. Note that reduction of the alkyne is slower than reduction of the alkenes, even though alkyne reduction is generally more exothermic than alkene reduction.[31] This suggests that the difference in reactivity between the alkynes and alkenes is a consequence of kinetic control of reactivity under the experimental conditions. Differences in rates of reaction of alkenes and alkynes in various addition reactions are often observed under conditions closer to ambient, and are attributed to the kinetic stability of the π-bond electrons in alkynes compared to alkenes. This is generally assumed to be a consequence of a shorter overall bond between the sp-hybridized carbons of the alkyne.[31] Slower hydrogenation of alkynes compared to alkenes on a metal catalyst has been observed previously, and assigned to
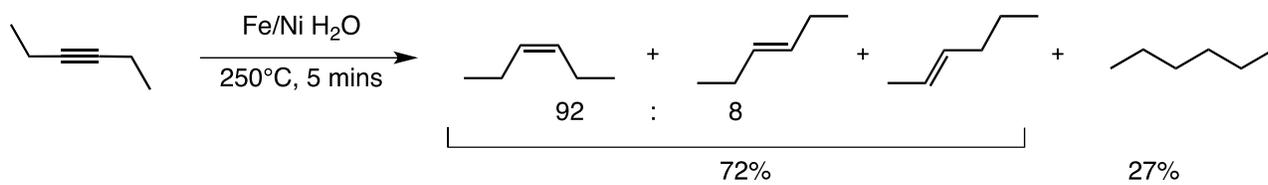
Scheme 4. Products observed for the hydrothermal reduction of 3-hexyne with iron and nickel at 250°C after 5 minutes.

differences in the adsorption of the two functional groups to the surface of the catalyst.[32]

Reduction of 3-hexyne was also studied further to explore the stereochemistry of the hydrothermal hydrogenations, Scheme 4. The smaller ethyl substituents on the 3-hexyne compared to the phenyl rings on **DPA** could result in changes in the adsorption of the alkyne to the catalytic surface compared to **DPA**, which in turn could influence the rate of reaction or the reaction stereochemistry. Indeed, reduction of 3-hexyne was observed to be much faster than reduction of **DPA**. Conversion of 3-hexyne into products was >95% complete after only 5 minutes compared to ~13% conversion of **DPA** after the same time period. The reaction mixture after this time period consisted of 72% alkenes and 27% hexane, Scheme 3. Of the alkenes, 68% was *cis*-3-hexene, 6% t*rans*-3-hexene, and 26% was *trans*-2-hexene. The primary 3-hexene products were formed in a *cis*-/*trans*- ratio of 92:8, which is even larger than that found for reduction of **DPA**. These results suggest that hydrogen addition is *syn*-, and that the preference for *syn*-addition depends to some extent on molecular structure.

Electron Donating and Withdrawing Substituent Effects

The mechanistic studies described so far are consistent with a conventional Horiuti-Polyani mechanism for hydrogenation at a metal surface.[33] The reaction conditions, however are reminiscent of several dissolving metal reductions, in which the hydrogen atoms are produced by a metal that formally provides the electron and a Brønsted acid that formally provides a proton.[34] In dissolving metal reductions the electron and proton transfer processes are often sequential. Specifically, electron transfer is often a first step, forming a radical anion that is subsequently protonated. Alternatively, the substrate could be protonated first, and then accept an electron. At the reaction temperature, the pK_w is ca. 11, compared to ca. 14 at ambient, i.e., the water

autoionizes more efficiently.[7] Therefore, the hydronium concentration is higher, and together with the higher thermal energy, proton transfer reactions can occur that would not otherwise be expected in water at ambient temperature and pressure (see, for example, ref 10). Although molecular hydrogen is clearly formed when iron is heated to 250°C, in the presence of an organic substrate an electron/proton transfer mechanism at the metal surface may compete with molecular hydrogen formation and contribute to the overall reduction process.

The electron/proton transfer mechanisms common in dissolving metal reductions have ionic intermediates.[34] Evidence for ionic intermediates in a mechanism can be obtained from studies of the influence of electron donating and withdrawing substituents. For example, in a recent study of the reduction of styrenes using a homogeneous iron-based catalyst, styrenes with electron withdrawing substituents were found to reduce much slower than those with donating groups. A Hammett plot of the kinetic data was consistent with a proposed mechanism involving rate-determining hydride transfer to form an intermediate that has a formal negative charge on the benzylic carbon.[35] We looked for similar substituent effects on the rates of the present reductions.

Hydrothermal reduction of styrene was performed as described above and compared to the corresponding reduction of *p*-methoxystyrene and *m*-trifluoromethylstyrene. Reaction of all three styrenes resulted in formation of the corresponding ethylbenzene as the only detectable product (92-99% chemical yield), Figure 4. Reaction was complete within 15 minutes for each styrene. The kinetics of the reactions were determined from concentration versus time data, Figure 4. For *m*-trifluoromethylstyrene, a steady-state was reached at 93% conversion whereas for the other styrenes no starting material could be detected using our method of analysis. That the *m*-trifluoromethylstyrene reaction reached a steady-state may be a consequence of the strong
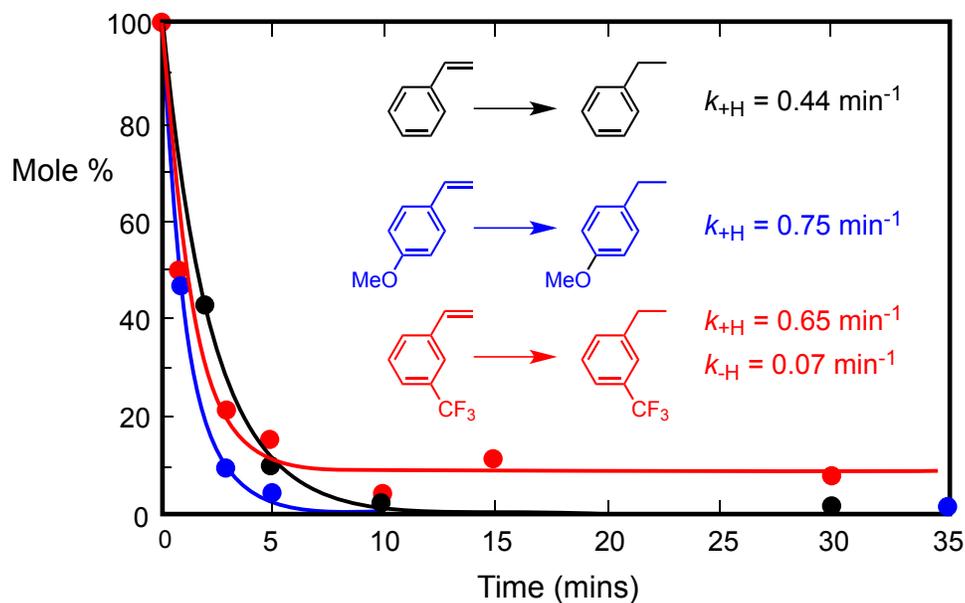
Fig 4. Kinetics of addition of hydrothermal reduction of three styrenes. The curves are best fits to the experimental data (symbols) according to pseudo-first order kinetics. The pseudo-first order rate constants for reduction (addition of hydrogen) are k_{+H}. For *m*-trifluoromethylstyrene a steady-state can be observed, therefore the rate constant for dehydrogenation (removal of hydrogen), k_{-H}, can also be determined. The uncertainties in the rate constants are estimated to be ±15%, based on repeated measurements.

electron withdrawing substituent stabilizing the vinyl π-bond. The pseudo-first order rate constants for addition of hydrogen to the styrenes to form the ethylbenzenes, k_{+H}, and the pseudo-first order rate constant for the reverse reaction for m-trifluoromethylstyrene, k_{-H}, were determined by fitting the data according to first order kinetics, and are summarized in Figure 4.

Both the electron donating and withdrawing groups increase the rate of reduction compared to the parent styrene, k_{+H}, although we note the effects are small: factors of 1.5 and 1.7 for the withdrawing and donating substituents, respectively. This argues strongly against an ionic intermediate playing any substantial role in the reaction, since the substituent effects would be expected to be much larger and in opposite directions if that were the case. At the very least, the formations of ionic intermediates are not connected to the rate determining steps in the reactions.

If benzylic radical intermediates were to be formed in a rate-determining steps then the substituent effects would be expected to be even smaller due to the absence of charge. However, the data are also not consistent with formation of radical intermediates, since it has been shown that a m-trifluoromethyl substituent destabilizes a benzyl radical,[36] in which case reduction should be slower for the m-trifluoromethylstyrene, and we observe the opposite effect. In addition, no coupling or disproportionation products could be detected in any of the reduction reactions, arguing against the formation of freely diffusing radicals.

The stereochemical and electronic probes of the mechanism are consistent with reaction *via* conventional metal-catalyzed formation of carbon-hydrogen bonds at the metal surface after dissociative adsorption of hydrogen and the substrate to the metal surface.[33,37] In one detailed kinetic study of hydrogenation of styrene on palladium particles the authors concluded that insertion of the first hydrogen atom was an important contributing factor to the overall rate of reaction.[38] Information on the relative rates of reduction of the various structures included in this

work is summarized in Table 1, as the first half lives of the reactions under the same conditions. These half-lives vary over roughly an order of magnitude. In principle, it should be possible to find conditions in which one functional group could be reduced in the presence of another, if their relative rates of reaction differ by one order of magnitude. However, the observed behavior of the functional groups shows that the situation is not so simple. The alkyne **DPA** is the slowest to react, slower than any of the alkenes, but the alkyne 3-hexyne reacts much more quickly, faster than many of the alkenes. The rates of hydrogenation of π-bonds on metal surfaces are determined by a complex interplay between rates of chemisorption, desorption, and the rate of hydrogen atom transfer to the alkene in the chemisorbed state.[33,37] It is not obvious how to predict relative rates of reactions *a priori* and thus predicting conditions for selective reduction of the π-bonds in these kinds of structures is not possible at this time.

Reaction Selectivity

Reduction of styrene shows that reduction of simple carbon-carbon double bonds can be accomplished in the presence of an aromatic ring. Benzene rings can, however, be reduced all the way to cyclohexane under hydrothermal conditions on much longer timescales, Scheme 5. At 250°C and 40 bars, complete reduction to cyclohexane requires 9 days. A pseudo-first order reaction rate constant of 2.4×10^{-4} min^{-1} can be determined from time-dependent concentration data collected over this time period (data not shown), Scheme 5. Slow reduction of benzene is not surprising due to well-known low-reactivity of the aromatic ring, and because the reaction presumably proceeds via a cyclohexadiene, which itself is a known hydrogen atom donor that releases molecular hydrogen to reform benzene.[39] Cyclohexadiene or cyclohexene cannot be detected by gas

Table 1. First half-lives for reduction at 250°C and 40 bar in water in the presence of iron and nickel[a]
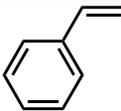
Substrate	$t_{1/2}$ **(min)**
	1.6 ± 0.2
	1.0 ± 0.2
	0.9 ± 0.2
	4 ± 2.0
	< 5
	6.3 ± 1.0
	7.5 ± 1.0
	18 ± 1.5
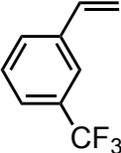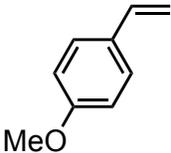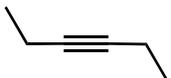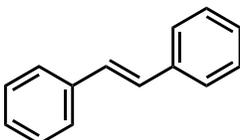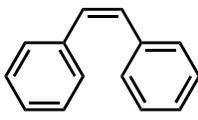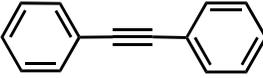
[a] The first half-lives and their uncertainties are derived from the rate constants obtained from analysis of time-dependent concentration data, see Figs 2 and 3 and Scheme 3. For cyclohexene, the half-life estimate is based on one experiment take to 55% conversion, the uncertainty in this case is based on analysis of the reproducibility of repeated measurements. For 3-hexyne the half-life of <5 mins is based on experiments that show >95% conversion in this time period.

2
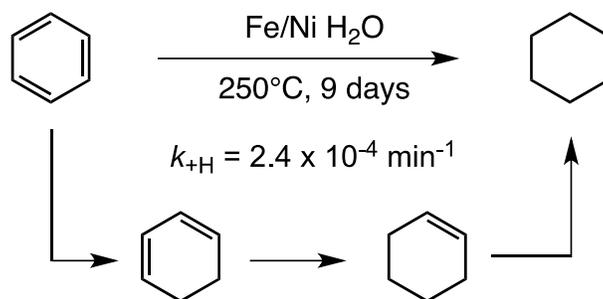
Scheme 5. Proposed pathway for hydrothermal hydrogenation of benzene; note the diene and alkene structures cannot be isolated. Conversion of benzene into cyclohexane is observed only after 9 days. The uncertainty in the pseudo-first order reaction rate constant, k_{+H}, is estimated to be ±15%.

Table 2. Selective hydrothermal reductions with iron and nickel at 250°C

Starting Compound	Major Product	Reaction Time	Conversion (%)	Selectivity (%)
		1 hour	100	95
		15 min	93	97
		70h	82	70
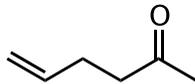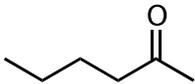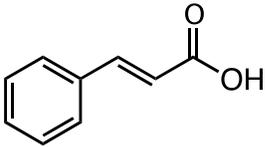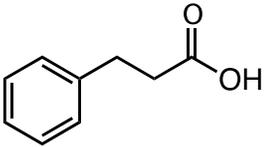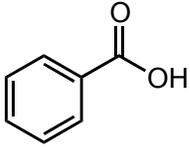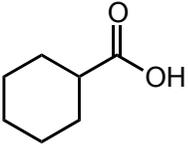
chromatographic analysis of the products at any time during this slow reduction.

Excellent selectivity towards reduction of carbon-carbon double bonds was observed in the presence of ketones and carboxylic acids, Table 2. Specifically, reaction of hex-5-en-2-one for one hour resulted in 100% conversion of the starting material, with 95% of the products being 2-hexanone, the other 5% was 2-hexanol, a follow-up reduction of 2-hexanone. Similarly, reaction of *trans*-cinnamic acid for only 15 minutes resulted in 93% conversion to hydrocinnamic acid, with 97% selectivity towards reduction of the carbon-carbon double bond, Table 2. The other 3% of the products were alcohols, formed in an alternative reduction pathway of the acid. Reduction of a benzene ring in the presence of a carboxylic acid function group was also observed. Benzoic acid could be reduced to cyclohexanecarboxylic acid with 80% conversion after 70 hours and 70% selectivity towards complete reduction of the benzene ring. Selectivity was lower than in the other reactions; nevertheless, this could still be a useful reaction since this particular ring reduction is generally only been observed only on Ru, Pd, and Rh catalysts.[40]

Conclusions

Selective reductions of carbon-carbon π-bonds can be accomplished under mild hydrothermal conditions related to those of geochemical reactions occurring deep in the Earth's crust.. The required pressure is not particularly high compared to many industrial processes: it is simply the water vapor pressure at the experimental temperature. The reducing agent is metallic iron, the only solvent is water and the nickel catalyst can be used in the form of a simple powder, i.e. no further processing is required such as is required to produce Raney Nickel.[41] Nickel is relatively inexpensive and has a much lower depletion risk than the rare metals conventionally used for

catalytic hydrogenation.[15,42] Many of the reactions described here are complete in less than one hour, even though no optimization of the catalyst structure or surface area has been attempted. This suggests there is potential to further optimize the catalyst and the reaction conditions, such as temperature. Both chemoselectivity and stereoselectivity are observed in the reactions, showing that the high temperature conditions do not result in non-selective reactivity.

Stereochemical, electron-donating, and electron-withdrawing probes of the mechanism are consistent with a conventional Horiuti-Polyani mechanism for the addition of two hydrogen atoms across a carbon-carbon multiple bond for a dissociatively adsorbed substrate and molecular hydrogen.

Further exploration of hydrothermal organic reactions under conditions that are traditionally relevant to geochemistry, geomimicry, is likely to uncover more useful reactions that are benign and use Earth abundant reagents and catalysts because this is the way that the Earth does chemistry. Like to the more established biomimicry, geomimicry offers new routes to organic chemicals that are robust, cost efficient, and amenable to being performed at a large scale.

References

1   P. Falkowski, R J. Scholes, E. Boyle, J. Canadell, D. Canfield, J. Elser, N. Gruber, K. Hibbard, P. Högberg, S. Linder, F.T. Mackenzie, B. Moore III, T. Pedersen, Y. Rosenthal, S. Seitzinger, V. Smetacek, W. Steffen, *Science*, 2000, **290**, 291.

2   (a) J. S. Seewald, *Nature*, 2003, **426**, 327; (b) H. C. Helgeson, L. Richard, W.F. McKenzie, D.L. Norton, A. Schmitt A, *Geochim Cosmochim Acta*, 2009, **73**, 594; (c) B. Horsfield, H.J. Schenk, K. Zinka, R. Ondraka, V. Dieckmanna, J. Kallmeyera, K. Mangelsdorfa, R. di Primio, H. Wilkes, R.J. Parkes, J. Fry, B. Cragg, *Earth Planet Sci Lett.*, 2006, **246**, 55; (d) J. P. Amend, T.M. McCollom, M. Hentscher, W. Bach, *Geochim Cosmochim Acta*, 2011, **75**, 5736.

3   (a) Z. Yang, I.R. Gould, L.B. Williams, H.E. Hartnett, E.L. Shock, *Geochim. Cosmochim. Acta*, 2018, **223**, 107; (b) J. A. Shipp, I.R. Gould, E.L. Shock, L.B. Williams, H.E. Hartnett, *Proc. Natl. Acad. Sci.*, 2014, **111**, 11642; (c) Z. Yang, I.R. Gould, L.B. Williams, H.E. Hartnett, E.L. Shock, *Geochim. Cosmochim. Acta*, 2012, **98**, 48; (d) J. A. Shipp, I.R. Gould, P. Herckes, E.L. Shock, L.B. Williams, H.E. Hartnett, *Geochim. Cosmochim. Acta*, 2013, **104**, 194.

4   (a) M. Siskin, A.R. Katritzky, *Science* 1991, **254**, 231; (b) A. R. Katritzky, S.M. Allin, M. Siskin, *Acc. Chem. Res.* 1996, **29**, 399; (c) A. R. Katritzky, D.A. Nichols, M. Siskin, R. Murugan, M. Balasubramanian, *Chem. Rev.* 2001, **101**, 83; (d) M. Siskin, A.R. Katritzky, *Chem. Rev.* 2001, **101**, 825; (e) N. Akiya, P.E. Savage, *Chem. Rev.* 2002, **102**, 2725; (f) S. E. Hunter, P.E. Savage, *Chem. Eng. Sci.* 2004, **59**, 4903.

5   (a) P. Körner, D. Junga, A. Kruse, *Green Chem.*, 2018, **20**, 2231; (b) Z. Liu, G. Tian, S. Zhu, C. He, H. Yue, S. Feng, *ACS Sustainable Chem. Eng.*, 2013, **1**, 313; (b) S. Avola, M.

Guillot, D. da Silva-Perez, S. Pellet-Rostaing, W. Kunz, F. Goettmann, *Pure Appl. Chem.* 2013, **85**, 89; (c) K. Shanab, C. Neudorfer, E. Schirmer, H. Spreitzer, *Curr. Org. Chem.* 2013, **17**, 1179. (b) S.E. Hunter, P.E. Savage, *Chem. Eng. Sci.* 2004, **59**, 4903-4909. (c) S.E. Hunter, C.A. Felczak, P.E. Savage, *Green Chem.* 2004, **6**, 222-226. (x) D. Broll, C. Kaul, A. Kramer, P. Krammer, T. Richter, M. Jung, H. Vogel, P.D. Zehner, *Angew. Chem. Int. Ed Engl.* 1999, **38**, 2998-3014.

6   J. W. Johnson, D. Norton, *Am. J. Sci.* 1991, **291**, 541.

7   A. H. Harvey, D. G. Friend, in *Aqueous Systems at Elevated Temperatures and Pressures*, eds. D. A. Palmer, R. Fernandez-Prini, A.H. Harvey, Elsevier: San Diego, CA, 2004.

8   (a) K. J. Robinson, I.R. Gould, K.M. Fecteau, H.E. Hartnett, L.B. Williams, E.L. Shock, *Geochim. Cosmochim. Acta*, 2019, **244**, 113; (b) S. Venturi, F. Tassi, I.R. Gould, E.L. Shock, H.E. Hartnett, E.D. Lorance, C. Bockisch, K.M. Fecteau, F. Capecchiacci, O. Vaselli, *J. Volcan. Geotherm. Res.*, 2017, **346**, 21; (c) Z. Yang, E.D. Lorance, C. Bockisch, L.B. Williams, H.E. Hartnett, E.L. Shock, I.R. Gould, *J. Org, Chem.* 2014, **79**, 7861.

9   Z. Yang, H.E. Hartnett, E.L. Shock, I.R. Gould, *J. Org. Chem.* 2015, **80**, 12159.

10   C. Bockisch, E.D. Lorance, H.E. Hartnett, E.L. Shock, I.R. Gould, *ACS Earth Space Chem.*, 2018, **2**, 821.

11   (a) C. P. Horwitz, in *Innovations in Green Chemistry and Green Engineering*, eds. P. Anastas, J. Zimmerman, Springer: New York, NY, 2013; (b) C.-J. Li, B.M. Trost, *PNAS*, 2008. **105**, 13197; (c) R. A. Sheldon, I.W. Arends, G.J. Ten Brink, A. Dijksman, *Acc. Chem. Res.*, 2002, **35**, 774.

12   (a) P. Gallezot, P. *Chem. Soc. Rev.* 2012*,* **41**, 1538. (b) D. D. Laskar, B. Yang, H. Wang

and J. Lee, Biofuels, *Bioprod. Biorefin.*, 2013, **7**, 602. (c) C. Zhang, J. Xing, L. Song, H.

Xin, S. Lin, L. Xing and X. Li, *Catal. Today*, 2014, **234**, 145–152.

13   (a) M. Aresta, A. Dibenedetto, *Catal. Today,* 2004, **98**, 455. (b) A. R. Paris, A.B. Bocarsly,

ACS Catal., 2017, **7**, 6815– 6820. (c) M. D. Sampson, C.P. Kubiak, *J. Am. Chem. Soc.*

2016, **138**, 1386.

14   (a) M. R. Arnold, *Ind. Eng. Chem.*, 1956, **48**, 1629. (b) V. K. Ahluwalia, *Reduction in*

Organic Synthesis, 1st Ed.; CRC Press: Boca Raton, Fl, 2012; (c) M. Hudlický, *Reductions*

in Organic Chemistry; American Chemical Society: Washington, D.C., 1996; (d) P. N.

Rylander, in *Ullmann's Encyclopedia of Industrial Chemistry*; Wiley-VCH: Weinheim,

2005.

15   Risk List 2015; British Geological Survey (National Environmental Research Council):

Nottingham, UK, 2015.

16   P.N. Rylander, *Catalytic Hydrogenation in Organic Chemistry*. Academic Press: New

York, 1979.

17   (a) X. Cui, H. Yuan, K, Junge, C. Topf, M. Beller, F. Shi, *Green Chem*. 2017, **19**, 305; (b)

C. Lucarelli, A. Lolli, A. Giugni, L. Grazia, S. Albonetti, D. Monticelli, A. Vaccari, *Appl.*

Catal., B 2017, **203**, 314; (c) V. K. Soni, P.R. Sharma, G. Choudhary, S. Pandey, R.K.

Sharma, *ACS Sustainable Chem. Eng.* 2017, **5**, 5351.

18   R. J. Press, K.S.V. Santhanam, M.J. Miri, A.V. Bailey, G.A. Takacs, *Introduction to*

Hydrogen Technology, Wiley, Hoboken, NJ, 2009, Ch. 4.1, p. 195.

19   (a) M.A. Keane, M. Li, L. Collado, F. Cardenas-Lizana, *React. Kin. Mech. Cat.* 2018, **125**,

25-36. (b) S. Werkmeister, J. Neumann, K. Junge, M. Beller, *Chem. A Eur. J* 2015, **21**,

12226–12250. (c) M. Trincado, D. Banerjee, H. Grutzmacher, *Energy Environ. Sci.* 2014, **7**, 2464–2503. (d) A. Bohre, S. Dutta, B. Saha, M.M. Abu-Omar, *ACS Sustain. Chem. Eng.* 2015, **3**, 1263–1277. (e)Shiraishi, Y., Hirai, T. J. Photochem. Photobiol. C 2008, **9**, 157–170.

20   C. Schafer, C.J. Ellstrom, H. Cho, B. Torok, *Green Chem.* 2017, **19**, 1230.18.

21   (a) Y.-P. Sun, X.-Q. Li, J. Cao, W.-X. Zhang, H.P. Wang, *Adv. Coll. Inter. Sci.*, 2006, **120**, 47. (b) B. Gu, L. Liang, M.J. Dickey, X. Yin, S. Dai, *Environ. Sci. Technol.* 1998, **32**, 3366. (c) F. Fua, D. Dionysios, H. L. Dionysioub, *J. Haz. Mat.* 2014, **267**, 194.

22   A. Agrawal, A.G. Tratnyek, *Environ. Sci. Technol.* 1996, **30**, 153.

23   (a) J.W. Johnson, E.H. Oelkers, H.C. Helgeson, *Comp. Geosci.* 1992, **18**, 899. (b) E. L. Shock, H.C. Helgeson, *Geochim. Cosmochim. Acta* 1990, **54**, 915. (c) E. L. Shock, E.H. Oelkers, J.W. Johnson, D.A. Sverjensky, H.C. Helgeson, *J. Chem. Soc., Faraday Trans.* 1992, **88**, 803.

24   H. C. Helgeson, J.M. Delany, H.W. Nesbitt, D.K. Bird, *Am. J. Sci* 1978, **278-A**, 1-229.

25   R. A. Robie, B.S. Hemingway, J.R. Fisher, *Thermodynamic Properties of Minerals and Related Substances at 298.15 K and 1 Bar (10^5 Pascals) Pressure and at Higher Temperatures*, Government Printing Office, Washington DC, 1978, p 456.

26   K. K. Kelley, *Data on theoretical metallurgy. XIII. High-Temperature, Heat-Capacity, and Entropy Data for the Elements and Inorganic Compounds*. U.S. Bur Mines Bull, 1960, No. 584, p 232.

27   (a) K. Son, J.L. Gland, *J. Phys Chem B*, 1997, **101**, 3540. (b) B. B, Corson, V.N. Ipatieff, *J. Am. Chem. Soc.* 1939, **61**, 1056.

28 (a) F. Alonso, I. Osante, M. Yus, *Tetrahedron* 2007, **63**, 93. (b) V. Mintsa-Eya, L. Hilaire, A. Choplin, R. Touroude, F.G. Gault, *J. Catal.* 1983, **82**, 267. (c) S. Mitsui, K. Gohke, H. Saito, A. Nanbu, Y. Senda, *Tetrahedron* 1973, **29**, 1523. (d) S. Mitsui, S. Imaizumi, A. Nanbu, Y. Senda, *J. Catal.* 1975, **36**, 333.

29 S. Nishimura, H. Sakamoto, T. Ozawa, *Chem. Lett.* 1973, 855-8.

30 S Hoops, S. Sahle, R. Gauges, C. Lee, J. Pahle, N. Simus, M. Singhal, L. Xu, P. Mendes, U. Kummer, *Bioinformatics* 2006, **22**, 3067.

31 P. Y. Bruice, *Organic Chemistry, 8th Ed.*. Pearson; Upper Saddle River, NJ, 2015.

32 G. J. Kubas, *Metal Dihydrogen and σ-Bond Complexes*, Kluwer Academic/Plenum Publishers: New York, 2001

33 J. Horiuti, M. Polanyi, *Trans. Faraday Soc.* **1934**, *30*, 1164.

34 Huffman, J. W., in *Comprehensive Organic Synthesis, Vol. 8*, eds. B. M. Trost, I. Fleming, Pergamon Press, Oxford, UK, 1991.

35 R. Xu, S. Chakraborty, S.M. Bellows, H. Yuan, T.R. Cundari, W.D. Jones, *ACS Catal.* **2016**, *6*, 2127.

36 J. M. Dust, D.R. Arnold, *J. Am. Chem. Soc.* 1983, **105**, 1221.

37 J. H. Brewster, *J. Am. Chem. Soc.* **1954**, *76*, 6361-3.

38 C. Betti, J. Badano, C. Lederhos, M. Maccarrone, N. Carrara, F. Coloma-Pascual, M. Quiroga, C. Vera, *React. Kinet., Mech. Catal.* **2016**, *117*, 283.

39 S. W. Benson, R. Shaw, *J. Am. Chem. Soc.* **1967**, *89*, 5351.

40 (a) Y. Tang, S. Miao, H.N. Pham, A. Datye, X. Zheng, B.H. Shanks, *Appl. Catal. A* **2011**, *406*, 81. (b) Y. Wei, B. Rao, X. Cong, X. Zeng, *J. Am. Chem. Soc.* **2015**, *137*, 9250. (c) J.

A. Anderson, A. Athawale, F.E. Imrie, F. McKenna, A. McCue, D. Molyneux, K. Power, M. Shand, R.P.K. Wells, *J. Catal.* **2010***, 270*, 9.

41   T.-K. Yang, D.-S. Lee, J. Haas, *Encyclopedia of Reagents for Organic Synthesis*; Wiley: New York, 2005.

42   B. Su, Z.-C. Cao, Z.-J Shi, *Acc. Chem. Res.*, 2015, **48**, 886–896

TABLE OF CONTENTS GRAPHIC